Roquin1 Suppresses Breast Cancer Growth by Inducing Cell Cycle Arrest via Selectively Destabilizing Cell Cycle–Promoting Gene mRNAs

Wenbao Lu (luwenbao_217@imc.pumc.edu.cn)
Insitute of Microcirculation
Meicen Zhou
Beijing Jishuitan Hospital
Bing Wang
Chinese Academy of Medical Sciences and Peking Union Medical College
Xueting Liu
Chinese Academy of Medical Sciences and Peking Union Medical College
Bingwei Li
Chinese Academy of Medical Sciences and Peking Union Medical College

Research

Keywords: Roquin1, breast cancer, cell cycle, Cyclin E1, MCM2, mRNA decay

Posted Date: August 5th, 2020

DOI: https://doi.org/10.21203/rs.3.rs-53499/v1

Version of Record: A version of this preprint was published on November 23rd, 2020. See the published version at https://doi.org/10.1186/s13046-020-01766-w.

Abstract

Background: Dysregulation of cell cycle progression is one of the common features of human cancer cells, however, its mechanism remains unclear. This study aims to clarify the role and the underlying mechanisms of Roquin1 in cell cycle arrest induction in breast cancer.

Methods: Public cancer databases were analyzed to identify the expression pattern of Roquin1 in human breast cancers and the significant association with patient survival. Quantitative real-time PCR and western blots were performed to detect the expression of Roquin1 in breast cancer samples and cell lines. Cell counting, MTT assay, flow cytometry, and in vivo study were conducted to investigate the effects of Roquin1 on cell proliferation, cell cycle progression and tumor progression. RNA-sequencing was applied to identify the differential genes and pathways regulated by Roquin1. RNA immunoprecipitation assay, luciferase reporter assay, mRNA half-life detection, RNA affinity binding assay, and RIP-ChIP were used to explore the molecular mechanisms of Roquin1.

Results: We showed that Roquin1 expression in breast cancer tissues and cell lines was inhibited, and the reduction in Roquin1 expression was associated with poor overall survival and relapse free survival of patients with breast cancer. Roquin1 overexpression inhibited breast cancer cell proliferation and induced G1/S cell cycle arrest without causing significant apoptosis. In contrast, knockdown of Roquin1 promoted breast cancer cell growth and cycle progression. Moreover, in vivo induction of Roquin1 by adenovirus significantly suppressed breast tumor growth and metastasis. Mechanistically, Roquin1 selectively destabilizing cell cycle–promoting genes, including Cyclin D1, Cyclin E1, cyclin dependent kinase 6 (CDK6) and minichromosome maintenance 2 (MCM2) through targeting the stem–loop structure in the 3’untranslated region (3’UTR) of mRNAs via its ROQ domain, leading to the downregulation of cell cycle–promoting mRNAs.

Conclusions: Our findings demonstrated that Roquin1 was a novel breast tumor suppressor and could induce G1/S cell cycle arrest by selectively downregulating the expression of cell cycle–promoting genes, which might as a potential molecular target for breast cancer treatment.

Background

Cell cycle dysregulation is a common feature of human cancers, characterized by uncontrolled cell proliferation and cell cycle progression of cancer cells [1–3], which is one of the reasons why tumor cells are capable of unlimited proliferation and resistance to conventional treatments. Although increasing understanding has expanded the knowledge on cell cycle regulation, the post-transcriptional mechanism of cell cycle dysregulation in cancer cells, especially through RNA-binding proteins (RBPs), remains unclear.

Roquin1, a Cys-Cys-Cys-His-type RBP encoded by the *Rc3h1*, is initially found to play an important role in immune regulation with its ubiquitin ligase activity [4, 5]. Roquin1 is rapidly induced in T cells upon stimulated by the inflammatory inhibitory factor Interleukin-10 [6]. Furthermore, Roquin1 can suppress

autoimmunity by destabilizing the inducible T cell costimulator (ICOS) mRNA through its ROQ domain [7]. Therefore, Roquin1 is regarded as a regulator of immune system and orchestrate the differentiation of various immune cells, including Follicular helper T cell (TfH), Natural killer T (NkT), and Regulatory T (Treg) cells [8–10]. Roquin1 deficiency induces the death of mouse embryos and severe autoimmune reaction and enteritis [11, 12]. Evidence showed that Roquin1 could decay mRNA by binding the stem–loop structure in the 3'UTR of target genes [13–15]. Besides, Roquin1 serves as a regulator of multiple signaling pathways, such as AMP-activated protein kinase (AMPK) [16], NF-κB [17], and PI3K-mTOR [18], to regulate immune responses. Roquin1 is additionally able to regulate microRNA homeostasis [19]. In cancerous TfH cells, *Roquin1* expression level is similar to that in normal TfH cells [20]. However, it remains unknown whether Roquin1 plays a role in cancer progression.

In this study, we identified that Roquin1 is a potent breast tumor suppressor by inducing tumor cell cycle arrest through selectively suppressing the expression of cell cycle–promoting genes, including *CCND1*, *CCNE1*, *CDK6*, and *MCM2*. Roquin1 expression was reduced in breast cancer tissues and cells, which might contribute to their absence from cell cycle regulation. Ectopic Roquin1 expression induces G1/S cell cycle arrest in breast tumor cells. In contrast, further suppression of Roquin1 expression by shRNAs facilitates tumor cell proliferation and cell cycle progression. Consistent with these *in vitro* observations, Roquin1 expression *in vivo* significantly inhibits tumor growth and metastasis. By analyzing the database of human breast tumors [21], low Roquin1 levels in tumor samples were found to be strongly associated with poor survival of luminal A, luminal B, and Basal breast cancer patients. Moreover, Roquin1 expression is negatively correlated with *CCNE1* and *MCM2* in human breast tumors. These results suggested that Roquin1 was a potential tumor suppressor, which was involved in regulating cell cycle progression by suppressing the cell cycle–promoting genes expression.

Methods

Mice

6–8 female BALB/c nude mice were bought from the Institute of Laboratory Animal Science, Chinese Academy of Medical Sciences (CAMS) & Peking Union Medical College (PUMC). The mice were bred in cages with filter tops in a laminar flow hood in pathogen-free condition, with a 12 h light, 12 h dark cycle. All experimental procedures were approved by the Experimental Animal Care and Ethics Committee of the Institute of Microcirculation, CAMS & PUMC.

Cell lines and plasmids

The human breast cancer cell line (MDA-MB-231, MDA-MB-468, MCF7 and T47D), human normal mammary epithelial cell lines (MCF-10A and MCF-12A), human lung cancer cell line A549 cell, and human liver cancer cell line (HepG2) cells were obtained from the American Type Culture Collection (ATCC) and cultured in DMEM or RPMI-1640 with 10% FBS plus 1% Peni/Stro, respectively. HEK293 and HEK293T cells were obtained from National Infrastructure of Cell Line Resource (Beijing, China). The human full-length Roquin1 coding sequence (NM_172071) was synthesized, sequenced and inserted into

pEGFP-N1 vector at EcoR I and Age I sites. Roquin1 serial deletion plasmids were generated by inserting the PCR-amplified fragments into pEGFP-N1 vector at EcoR I and Age I sites. A set of luciferase reporters were constructed by inserting the full-length 3'UTRs of human *MCM2*, *Cyclin D1*, and *Cyclin E1* or part 3'UTR (1-1440 bp) of *CDK6* into the pGL3 control vector (Promega) between Xba I and Fse I sites, respectively. For stem-loop deletion reporters, point mutated and truncated *CCNE1*-3'UTR (1-256 bp) (Δstem-loop) and *MCM2*-3'UTR (1-360 bp) (Δstem-loop) were amplified, sequenced, and inserted into pGL3 control vector using Phusion Site-Directed Mutagenesis Kit (Thermo Scientific). For stem-loop insertion constructs, the stem-loop sequences of *CCNE1* 3'UTR (257–276) and *MCM2* 3'UTR (361–377) were inserted into pGL3-β-actin$^{3'UTR}$ reporter at 555 base pair.

Cell cycle analysis

Cells were trypsinized and washed twice with PBS, and then fixed in cold ethanol (70%). The cells were then stained with propidium iodide (20 μg/mL) and RNase A (0.2 mg/mL) for 30 min. The stained cells were analyzed by flow cytometry and the data were analyzed with FlowJo software.

RNA-sequencing analysis

MCF7/Roquin1-GFP, MDA-MB-468/Roquin1-GFP, A549/Roquin1-GFP, HepG2/Roquin1-GFP, and their control cells (expressing GFP) were cultured for 36 h and total RNA was extracted using the TRIzol method. RNA sequencing (RNA-seq) was completed by Allwegene Technology Inc., Beijing. The cDNA library was then constructed using polymerase chain reaction (PCR) amplification. RNA-seq was performed with the PE150 sequencing strategy using an Illumina second-generation high-throughput sequencing platform. RNA-seq reads with inferior quality or adapters were filtered. Clean read data were processed using Tophat2 and Cufflinks software to complete the alignment of transcriptomes. Genes not expressed in any sample were excluded from further analysis. Differentially expressed genes and transcripts were then filtered for false discovery rate (FDR)-adjusted *P* values less than or equal to 0.05.

Gene Ontology and Kyoto Encyclopedia of Genes and Genomes (KEGG) pathway analysis

RNA-seq data were deposited (PRJNA637876). The common up- and -downregulated mRNAs by Roquin1 in two breast cancer cells were classified using the Venn diagram. Gene Ontology (GO) (biological process) and KEGG pathway analyses of commonly downregulated genes were done using DAVID Bioinformatics Tools and Ingenuity Pathway Analysis.

RNA immunoprecipitation

Roquin1/GFP fusion protein was expressed in MDA-MB-468/Roquin1 cells, and then whole cell lysates were pre-cleared with isotype IgG, followed by incubation with anti-GFP antibody at 4℃ for 4 hrs. The protein-RNA complexes were then pulled down by protein G agarose beads (sc-2002, SantaCruz) and total RNA extracted with TRIzol, followed by detection of cell cycle-promoting genes with RT-PCR.

Luciferase reporter assays

Luciferase assay was performed as described previously [22]. pGL3 luciferase reporter constructs containing full-length or segment of 3'UTR of different genes were transfected into HEK293 cells along with Roquin1/GFP, aa 1-441 (contain RING, ROQ, zinc finger domains), aa 441–1133 (contain PRD), aa 174–326 (only contain ROQ domain), and GFP-control constructs, respectively. All transfections were conducted in triplicate and repeated at least three times. The luciferase activity was measured 36 h after transfection using a Dual-Luciferase Reporter Assay System (Promega).

mRNA stability

Roquin1/GFP was expressed in MDA-MB-468 cells, and then actinomycin D (ActD, 5 μg/mL) and 5, 6-dichlorobenzimidazole riboside (DRB, 5 μg/mL) were added to block *de novo* RNA synthesis. Total RNA was collected at indicated time points, and the relative mRNA level was analyzed by qPCR. The half-life of mRNA was determined by comparing with the levels of mRNA before adding ActD and DRB. The half-life of different genes in Roquin1 knockdown cells and their corresponding scrambled control cells was also tested as described earlier.

shRNA lentivirus

Two lentiviral shRNAs (NM_172071.1-3458s1c1; NM_172071.1-2032s1c1) targeting human Roquin1 mRNA and two lentiviral shRNAs targeting human MCM2 (NM_004526.2-2553s21c1) and Cyclin E1 (NM_001238.1-1149s1c1) were purchased from Sigma. A scramble control shRNA was used as a control. Lentiviral particles were packaged in HEK293T cells by co-transfecting shRNA-pLKO.1, pCMV-dR8.2, and pMD2.G constructs. After 48 h, virus supernatants were collected and centrifuged to discard cell debris, and then added to target cells with 1 μg/mL polybrene for overnight. After two rounds infection, the target cells were selected with puromycin (2.5 μg/mL) for two weeks, followed by further study.

Hematoxylin and Eosin (H&E staining)

Mouse lung tissues were immersed in 10% formalin for at least two weeks, and then stained with H&E staining. Zeiss Imaging System is used for visualizing of H&E sections.

Statistical analysis

Data in bar graphs represent mean ± SD of at least three biological repeats. Statistical analysis was performed using Student's t-test by comparing treatment versus vehicle control or otherwise as indicated. P-value < 0.05 was considered to be statistically significant.

Results

Roquin1 expression was reduced in breast cancer patients and was associated with poor survival

Roquin1 expression was first analyzed in the breast tumor database (www.oncomine.org). Low levels of Roquin1 were found in various breast cancers, including breast carcinoma, invasive ductal breast

carcinoma, and invasive mixed breast carcinoma, although a slightly high level in invasive lobular breast cancer tissues (Fig. 1a; Additional file 1: Figure S1A). Experimentally, Roquin1 mRNA expression was significantly reduced in breast tumors compared with normal tissues (Fig. 1b). Meanwhile, Roquin1 protein expression was also lower in randomly selected four pairs of breast cancer tissues than in their surrounding normal tissues (Fig. 1c). Moreover, Roquin1 expression was significantly repressed at both protein (Fig. 1d) and mRNA (Fig. 1e) levels in several human breast cancer cell lines compared with normal mammary gland epithelial cells. Notably, by surveying Roquin1 expression across a gene array dataset [21], we found that low Roquin1 expression in human breast tumor samples was strongly associated with poor overall survival and relapse-free survival of patients (Fig. 1f and 1 g). Furthermore, the levels of Roquin1 in breast tumors were also associated with patient survival in the Luminal A, Luminal B, and Basal-like subsets (Fig. 1h-j). Although no significant correlation was found between Roquin1 expression and patient survival in HER2 + subsets, a similar trend like another three subsets was found (Fig. 1k). These results suggested that Roquin1 was of great significance for the prognosis of patients with breast cancer. Besides, we also found that Roquin1 was suppressed in other types of human cancers, including lung cancer, ovarian cancer, gastric cancer, and bladder carcinoma (Additional file 1: Figure S1B-1E). Striking, Roquin1 expression levels also significantly correlated with the prognosis of patients with these above cancers and liver cancer (Additional file 1: Figure S1F-1J), indicating Roquin1 might be clinical predictive for multiple cancers.

Roquin1 inhibits cell growth by inducing G1-S phase cell cycle arrest in breast cancer cells

To determine Roquin1 function in breast cancer progression, Roquin1/GFP fusion protein was expressed in breast cancer cells MCF7 and MDA-MB-468, respectively, and identified by Western blot (Fig. 2a). When Roquin1 overexpression, we noticed that the proliferation (Fig. 2b, c) and activity (Fig. 2d, e) of breast cancer cells were considerably reduced. Similar results were also found in human lung cancer cell A549 and human liver cancer cell HepG2 with Roquin1 overexpression (Additional file 1: Figure S2A-2D). To determine whether Roquin1 inhibited cell proliferation by affected tumor cell cycle progression, we evaluated the effect of Roquin1 overexpression on cell cycle by flow cytometry (FCM). The G1 phase percentage of breast tumor cells was significantly increased in Roquin1-overexpressing cancer cells compared with the controls. Meanwhile, a significant decrease in S phase percentage was detected after Roquin1 overexpression. Similar results were also found in A549 and HepG2 cells with Roquin1 overexpression (Additional file 1: Figure S2G-2J). However, the G2 phase percentage of cells did not change consistently among tumor cells which might be due to different cell types (Fig. 2f, g; Additional file 1: Figure S2I-2J). These findings suggested that Roquin1 was able to induce the G1/S cell cycle arrest in breast tumor cells. Indeed, the protein levels of p21, a typical cell cycle inhibitor, were induced by Roquin1 in breast tumor cells (Fig. 2h, i), and A549, HepG2 cells (Additional file 1: Figure S2K-2L). To determine whether Roquin1 induced apoptosis in breast tumor cells, cleaved caspase3 and PARP1, two key apoptosis indicators, were detected by Western blotting. Roquin1 was not able to cause significant cleavages of pro-caspase3 and pro-PARP1 in breast tumor cells, although a slightly cleaved PARP1 was detected in MDA-MB-468 cells 72 h after Roquin1 overexpression (Fig. 2j, k), indicating Roquin1 did not

cause cell apoptosis in breast tumor cells. This detection was consistent with the observation that no obvious cell death occurred after Roquin1 overexpression during cell culture. Collectively, these data clearly demonstrate that Roquin1 induces G1/S cell cycle arrest of breast tumor cells.

Roquin1 selectively inhibited the mRNA expression of cell cycle–promoting genes through targeting 3'UTRs

Next, we identified the genes affected by Roquin1 using RNA-seq in Roquin1-overexpressing MCF7 and MDA-MB-468 cells. Venn diagrams showed that 6556 genes were common downregulated and 7067 genes were common upregulated in two breast tumor cells (Additional file 1: Figure S3A). We further focused on the expression of cell cycle–related genes. Interestingly, the genes that promote cell cycle progression, including G1/S transition, G2/M transition, S phase transition, and M phase transition, were suppressed, whereas the genes inhibiting cell cycle (*p21* and *Rb1*) were enhanced by Roquin1 in MCF7 (Fig. 3a) and MDA-MB-468 cells (Additional file 1: Figure S3B). Similar trends were also found in A549 and HepG2 cells (Additional file 1: Figure S3C-3D), indicating that Roquin1 could regulate the expression of cell cycle-related genes in tumor cells. Detailed RNA-seq data were summarized in Additional file 3: Table S1. Moreover, the 'cell cycle' pathway was the first of the top ten signaling pathways significantly enriched in the KEGG pathway analysis of downregulated genes (Fig. 3b). And, cell cycle–related terms 'cell division' and 'mitotic nuclear division' were enriched in the Gene Ontology (GO) analysis of downregulated genes (Fig. 3c). These computational analyses further supported our experimental findings. To validate the RNA-seq data, four downregulated cell cycle–promoting genes (i.e., *CCND1*, *CCNE1*, *CDK6*, and *MCM2*) and three upregulated cell cycle–inhibiting genes (i.e., *p21*, *p27*, and *Rb1*) were measured by real-time PCR. The mRNA expression of four cell cycle–promoting genes was reduced in a time-dependent manner by Roquin1 in breast cancer cells (Fig. 3d, e). Also, the protein levels of CCNE1 and MCM2 were downregulated by Roquin1 over time (Fig. 3f, g). However, the upregulated cell cycle–inhibiting genes without time-dependent changes (Additional file 1: Figure S3E). Notably, no time-dependent changes in the protein levels of p21 were observed in breast tumor cells (Fig. 2h, i). These results confirmed our RNA-seq data. In agreement with the overexpression results, the cell cycle–promoting genes were upregulated in Roquin1$^{San/San}$ MEF cells (Additional file 1: Figure S3F) [23], which further strengthened our findings. Taken together, these results indicate that Roquin1 regulates cell cycle pathway by inhibiting the mRNA expression of cell cycle-promoting genes.

As an RBP, we next examined whether Roquin1 binding to these cell cycle–promoting gene mRNAs. An RNA pull-down assay was performed with an anti-GFP antibody in Roquin1/GFP-expressing MDA-MB-468 cells, followed by detecting bound mRNAs by RT-PCR. Four cell cycle–promoting genes were amplified by PCR, whereas the GAPDH and cell cycle–inhibiting mRNAs were not amplified (Fig. 3h, i). *TNFα* was used as a positive control. These results indicated that Roquin1 selectively bound to the cell cycle-promoting genes but not cell cycle–inhibiting genes. To determine if the mRNA binding was mediated through 3'UTR, we cloned the 3'UTRs of *CCNE1*, *CCND1*, *CDK6* (part), and *MCM2* downstream of the luciferase gene as previously described [22], and then co-transfected these reporters with Roquin1 expression vector and its empty vector into HEK293 cells, followed by the measurement of luciferase activity. As shown in

Fig. 3J, Roquin1 significantly inhibited luciferase activities of all four 3'UTR reporters compared with cells transfected with control vector. The β-actin 3'UTR was used as a negative control. Collectively, these results suggested that Roquin1 specifically suppressed the mRNA expression of cell cycle–promoting genes by targeting their 3'UTRs.

Roquin1 destabilized the mRNAs of cell cycle–promoting genes via the ROQ domain

We speculated that Roquin1 might reduce cell cycle–promoting gene mRNAs through destabilizing the mRNAs. To confirm that, Roquin1/GFP was expressed in MDA-MB-468 cells and then *de novo* mRNA synthesis blocked using ActD (5 μg/mL) and DRB (5 μg/mL), followed by the measurement of the remaining mRNAs at different time points. The half-lives of indicated cell cycle–promoting mRNAs were shortened about 2-fold in Roquin1-overexpressing cells compared with cells expressing empty vector (Fig. 4a-d), while the half-lives of cell cycle–inhibiting mRNAs (including *p21*, *Rb1*, and *p27*) were barely affected by Roquin1 (Additional file 1: Figure S4A-4C), demonstrating that Roquin1 indeed inhibits cell cycle–promoting genes expression through the mRNA stability.

Roquin1 protein contains a RING finger, a ROQ domain, a zinc finger (ZF), and a proline-rich domain (PRD), of which the ROQ domain is involved in the destabilization of mRNAs [8]. To determine whether the ROQ domain is also responsible for the cell cycle–promoting mRNAs decay, a series of truncated Roquin1 mutants, including aa 1-441 containing RING, ROQ, and ZF domains, aa 441–1133 containing PRD domain, and aa 174–326 containing ROQ domain, were generated (Fig. 4e) and identified by Western blot analysis (Fig. 4f). Then, the mutants were co-transfected with wild-type (WT) Roquin1 as well as different 3'UTR reporters (Additional file 1: Figure S4D) into HEK293 cells. As shown in Fig. 4g and 4 h, WT, mutants aa 1-441 and aa174-326 suppressed the mRNA expression of four cell cycle–promoting genes and the luciferase activities of their 3'UTR reporters, but not mutant aa 441–1133, which was also consistent with the previous report [24]. In addition, aa 174–326 significantly inhibited the proliferation (Fig. 4i) and cell cycle progression (Fig. 4j; Additional file 1: Figure S4E) of MDA-MB-468 cells, which also signified that the ROQ domain in Roquin1 is essential for the induction of breast tumor cell cycle arrest.

Roquin1 knockdown stabilizes cell cycle–promoting gene transcripts and promotes tumor cell cycle progression

To further confirm the inductive effects of Roquin1 on tumor cell cycle arrest, we suppressed Roquin1 expression with two shRNAs in MDA-MB-231 cells, another triple-negative breast cancer cell. Roquin1 was reduced approximately 65% and 74% by #1shRNA and #2shRNA, respectively (Fig. 5a). Although Roquin1 is lowly expressed in breast tumors, the knockdown of Roquin1 considerably promoted the proliferation and activities of breast tumor cells (Fig. 5b, c), and increased the mRNA expression of cell cycle–promoting genes (Fig. 5d). These results were also consistent with previous data in Roquin1$^{san/san}$ MEF

cells [23]. However, depletion of Roquin1 had no effect on the mRNA levels of p21, Rb1, and p27 (Additional file 1: Figure S5A), again suggesting that Roquin1 directly suppressed the mRNA expression of cell cycle–promoting genes. Next, we examined the effect of Roquin1 knockdown on the half-life of cell cycle–promoting gene transcripts. As expected, reduced Roquin1 significantly prolonged the half-lives of the indicated cell cycle–promoting mRNAs (Fig. 5e-h). Furthermore, we also found reduced percentage of G1 phase cells and increased S phase cell percentage in MDA-MB-231 cells after knocking down Roquin1 (Fig. 5i; Additional file 1: Figure S5B). To confirm whether the cell cycle–promoting genes were involved in Roquin1-induced cell cycle arrest, CCNE1 and MCM2 were knocked down by shRNA lentivirus in Roquin1 knockdown MDA-MB-231 cells. Figure 5J showed that these shRNAs effectively knocked down *CCNE1* and *MCM2* expression. Upon co-knockdown of Roquin1 and CCNE1/MCM2, cell proliferation was closed to the scramble control compared to Roquin1 knockdown alone (Fig. 5k). Additionally, the percentage of G1 phase cells was significantly increased compared with the group of Roquin1 knockdown alone, and the percentage of S phase cells significantly decreased (Fig. 5l). Collectively, these results confirmed that Roquin1 repression indeed promotes breast tumor cell cycle progression through stabilizing cell cycle-promoting genes.

Roquin1 binds to the stem–loop structure of cell cycle-promoting genes for degradation

Roquin1 is known to degrade target mRNAs by binding to the stem–loop structure [14]. The 3'UTR sequences of four cell cycle–promoting genes were analyzed and a conserved sequence was identified across species, respectively, which could form a similar stem–loop structure (Additional file 1: Figure S6A-6D) using the RNAfold WebServer [25]. To investigate the role of the stem–loop structure in Roquin1-mediated degradation of cell cycle–promoting mRNAs, we generated deletion constructs by deleting the sequences containing the stem–loop in the 3'UTRs of *CCNE1* and *MCM2* (Fig. 6a). Then, full-length and deletion reporters with Roquin1 were co-transfected into HEK293 cells, followed by luciferase activity measurement. Roquin1 could significantly inhibit the luciferase activity of full-length *CCNE1* and *MCM2* 3'UTR, but not the deletion mutant reporters (Fig. 6b). In addition, Roquin1 reduced the activities of the reporters containing human β-actin 3'UTR with *CCNE1* or *MCM2* stem–loop structures, compared with that in the control group (Fig. 6c, d). These findings indicated that the stem-loop structure was pivotal for Roquin1-mediated cell cycle–promoting mRNAs decay.

To determine the necessity of stem–loop secondary conformation for mRNA degradation, two 3'UTR mutant reporters of CCNE1 and MCM2 were generated, of which the stem–loop structure of mutant1 was deleted by replacing two or four nucleotides and mutant2 retained the stem–loop structure after replacing four nucleotides (Fig. 6e). Subsequently, the two reporters were co-transfected with Roquin1 for measuring luciferase activity. Deletion of the stem–loop structure in the 3'UTRs of *CCNE1* and *MCM2* (mutant1) allowed them completely to resistant to Roquin1 inhibition, while the mutant2 that kept the stem–loop structure remained sensitive to Roquin1 suppression (Fig. 6f), indicating that the stem–loop structure in 3'UTRs was critical for cell cycle–promoting mRNAs decay. To further determine if Roquin1

physically bound to the stem–loop in the 3'UTRs of *CCNE1* and *MCM2*, we performed RNA affinity binding assay with biotin-labeled RNA probes. Wild-type RNA probes and mutant probes with the stem–loop structure either disrupted (mutant1) or retained (mutant2) were incubated with lysates of MDA-MB-468 cells expressing Roquin1/GFP fusion protein. Then, streptdavidin-coated magnetic beads were used for the pull-down assay, followed by Western blot detection with anti-GFP antibody. Roquin1/GFP fusion protein was pulled down by wild-type and mutant2 probes, but cannot by the stem–loop structure-deficient mutant1 probe (Fig. 6g), indicating that Roquin1 indeed interacted with the stem–loop structure of *CCNE1* and *MCM2 in vitro*. Furthermore, a modified RNA immunoprecipitation-chromatin immunoprecipitation (RIP-ChIP) assay was performed to verify that Roquin1 could bind the stem–loop structure *in vivo*. Roquin1/GFP fusion protein was expressed in MDA-MB-468 cells, the protein-RNA complex was pulled down by GFP antibody-coated beads, after the bound mRNAs sonicated, followed by amplification of the stem–loop sequences by RT-PCR. As expected, the stem–loop sequences in the 3'UTRs of *CCNE1* and *MCM2* could be amplified in the GFP antibody pull-down group, but not in the group using isotype IgG (Fig. 6h), indicating that the binding of Roquin1 to the 3'UTRs of cell cycle–promoting mRNAs inside breast tumor cells. Overall, these data demonstrate that Roquin1 recognized and bound to the stem–loop structure in the 3'UTRs of cell cycle–promoting genes for degradation.

Roquin1 suppressed breast tumor growth and metastasis

To determine the inhibitory effect of Roquin1 on breast cancer progression *in vivo*, MDA-MB-468/Roquin1-GFP cells (expressing the Roquin1/GFP fusion protein) and MDA-MB-468/GFP cells were inoculated into mammary gland fat pad of female nude mice (BALB/c). The growth and sizes of tumors expressing Roquin1/GFP fusion protein significantly reduced compared with the control tumors (Fig. 7a; Additional file 1: Figure S7A). Roquin1/GFP fusion protein expression in tumors was confirmed by the Western blot analysis (Fig. 7b). Meanwhile, a significant decrease in the number of metastatic foci (Fig. 7c) and metastatic white nodules (Additional file 1: Figure S7B) were observed in the lung tissues from Roquin1/GFP tumor-bearing mice. To avoid the impacts of the manual manipulation of gene expression and simulate the clinical treatment of breast cancer, adenoviruses expressing Roquin1/GFP fusion gene and its control virus (expresses GFP) were prepared to treat the established MDA-MB-231 breast tumors in nude mice. When tumor mass reaching approximately 5 mm in diameter, 10^{10} pfu of Roquin1/GFP adenovirus in 100 μL of PBS and the control adenovirus were injected every other day for five injections totally (Fig. 7d). Two days after injection, tumors began to shrink and grew slowly, while the tumors treated with control adenovirus continued growing well (Fig. 7e). At the end of the experiment, the sizes of tumors treated with Roquin1/GFP adenovirus were significantly smaller than those in the control group (Additional file 1: Figure S7C). Tumor metastasis was also significantly suppressed by Roquin1 adenovirus treatment (Fig. 7f; Additional file 1: Figure S7D). In line with the *in vitro* results, the protein levels of CCNE1 and MCM2 were also reduced in Roquin1 adenovirus-treated tumors (Fig. 7g), further confirming that Roquin1 suppressed the expression of cell cycle–promoting genes *in vivo*. Interestingly, the expression of *CCNE1* and *MCM2* was also significantly inhibited as *Roquin1* increased in 1,006 human breast cancer samples (Fig. 7h, i) (Additional file 4: Table S2) (Oncolnc.org/). Notably, higher levels of *CCNE1* and *MCM2* negatively correlated with poor survival of patients with breast cancer

(Fig. 7j, k). Conclusively, these findings strongly suggested that Roquin1 was a promising breast tumor suppressor, and the Roquin1-cell cycle-promoting genes axis might be considered as a new therapeutic target for breast tumor treatment in future.

Discussion

Currently, the role of Roquin1 in tumor progression is less reported. The analysis of the The Cancer Genome Atlas (TCGA) breast cancer databases showed that Roquin1 was expressed at low levels in human breast cancers. This low-level expression pattern was further confirmed in human breast cancer tissues and cell lines. And, low Roquin1 expression in tumors from various subtypes of breast cancer patients was strongly associated with poor survival signified the clinical significance of Roquin1. Despite no significant association in HER2 + breast cancer, the trend was similar to that of other subtypes. Besides, the levels of Roquin1 in several types of human cancers were also associated with patient survival, indicating that Roquin1 might be important for the prognosis of multiple types of human cancers.

We initially focused on the changes of cytokines secreted by tumor cells following Roquin1 overexpression in breast cancer cells. Unexpected, we found that Roquin1 significantly suppressed breast cancer cell proliferation and induced cell cycle arrest *in vitro*. To our knowledge, the relationship between Roquin1 and cell cycle progression has not been reported to date, especially in breast tumor progression. Using FCM, we found that Roquin1 could significantly stop G1/S transition in breast cancer cells as well as lung and liver cancer cells. However, we did not observe obviously cell apoptosis occurs after Roquin1 overexpression in breast tumor cells, which was different from the apoptosis induction role of another RBP, monocyte chemotactic protein-induced protein 1 (MCPIP1) in breast cancer progression [22]. Cell cycle arrest is triggered upon the balance between cell cycle–promoting and –inhibiting gene being broken. Our results clearly demonstrated that most of the genes that promoted cell cycle progression were downregulated by Roquin1, while those that inhibited cell cycle progression were upregulated. Indeed, four cell cycle-promoting genes were confirmed suppressed in a time-dependent manner but not the cell cycle–inhibiting genes. A selective targeting of Roquin1 to cell cycle–promoting mRNAs but not to cycle-inhibiting mRNAs might trigger an imbalance between cell cycle–promoting and inhibiting genes in tumor cells. Roquin1 also inhibits cell cycle progression in human liver cancer cells HepG2 and lung cancer cells A549, indicating that Roquin1 might be implicated in eliciting an antitumor response in a wide range of human cancers.

Among the Roquin1 target genes, *CCNE1*, *CCND1*, and *CDK6* are involved mainly in G1/S transition [26–28], while *MCM2* is important for DNA replication and S phase transition of cell cycle [29]. The broad targets of Roquin1 in the cell cycle pathway suggest that Roquin1 induces cell cycle arrest through targeting multiple molecules in breast tumor cells. We showed that Roquin1 suppresses the expression of these genes at the post-transcriptional level through enhancing mRNA degradation. The 3'UTR is important for the post-transcriptional regulation of genes. Many RBPs, including human antigen R (HuR) [30], tristetraprolin (TTP) [31], and MCPIP1, have been reported to regulate mRNA stability by the 3'UTR.

Indeed, Roquin1 inhibits luciferase activity through the 3’UTRs of cell cycle–promoting genes. It has been reported that the ROQ domain is essential for Roquin1-mediated mRNA degradation and immune regulatory effects [32]. We demonstrate that the ROQ domain is also required for the expression of cell cycle–promoting genes and cell cycle arrest induction by mutating the domains of Roquin1.

Many elements responsible for mRNA degradation are primarily localized in the 3'UTR, such as ARE, GU-rich element (GRE), and stem–loop structure [33–35]. Roquin is known to recruit other deadenylases to the 3’UTR for RNA decay by recognizing and binding the stem–loop structure [36]. Our results demonstrate that it is the stem–loop structure but not the ARE in the 3’UTRs is required for Roquin1-mediated cell cycle–promoting mRNAs decay. Roquin1 has been shown to bind a constitutive decay element (CDE) in the 3’UTR of TNFα mRNA and this CDE can fold into a stem–loop structure [37]. Indeed, we found a conserved consensus sequence was shared among different specifies in four cell cycle–promoting genes, respectively, and these sequences could fold into a stem–loop structure. Strikingly, no common stem–loop sequences were identified among four cell cycle–promoting genes, which support our hypothesis that Roquin1 mainly recognizes the secondary structure, instead of the linear sequence in the 3'UTR, which was also consistent with previous findings [13].

Finally, we proposed a model to elucidate the potential role of Roquin1 in the suppression of breast cancer cell cycle progression (Additional file 1: Figure S7E). Roquin1 selectively targeted cell cycle–promoting gene mRNAs for degradation via its ROQ domain by binding to the stem–loop structures in the 3'UTRs. As an RBP located in the cytoplasm, Roquin1 could regulate cell cycle progression by balancing the expression of cell cycle–related genes in tumor cells. Moreover, Roquin1 expression significantly negatively correlated with the expression of cell cycle–promoting genes in human breast tumors, further demonstrating the biological relevance of Roquin1 and the suppression of breast cancer. Our findings provided a novel regulator for cell cycle signaling pathway and also identified new target genes of Roquin1.

Conclusions

In summary, this study demonstrates that Roquin1 implicates in regulating the growth and metastasis of breast cancer by inhibiting cell cycle progression and proliferation. Roquin1 disrupts the balance of cell cycle signaling pathway by directly binding and destabilizing the cell cycle-promoting genes via the ROQ domain, which ultimately induced G1/S cell cycle arrest of breast cancer cells. Notably, low Roquin1 expression in breast tumors is strongly associated with poor survival of patients with breast cancer. Therefore, Roquin1 might be a new cell cycle suppressor in breast cancer, which could be a promising molecular target for tumor cell cycle-inhibiting therapy strategy.

Abbreviations

MTT: Thiazolyl Blue Tetrazolium Bromide; FCM: Flow cytometry; RIP-ChIP: RNA immunoprecipitation-chromatin immunoprecipitation; CCND1: Cyclin D1; CCNE1: Cyclin E1; CDK6: cyclin dependent kinase 6;

MCM2: Minichromosome maintenance 2; 3'UTR: 3'untranslated region; RBP: RNA-binding protein; RING: Really Interesting New Gene; ZF: zinc finger; ROQ: ROQ domain containing RNA binding activity; ATCC: American Type Culture Collection; RPMI 1640: Roswell Park Memorial Institute 1640; shRNA: short hairpin RNA; DMEM: Dulbecco's Modified Eagle's Medium; DRB: 5, 6-dichlorobenzimidazole riboside; ActD: Actinomycin D; ARE: AU-rich element; MEF: Mouse Embryonic Fibroblast.

Declarations

Acknowledgements

We thank all individuals who take part in this research.

Authors' contributions

WBL and MCZ were in responsible for the design of the study and wrote the manuscript; WBL participated in the RNA-seq analysis and bioinformatic analysis; MCZ performed qPCR and Western blot experiments; MCZ and BW contributed to culture of cells and in vitro cell assays; WBL, MCZ and BWL contributed to perform the study of the mechanism investigation; WBL, MCZ, and BWL were in charge of the animal experiments; XTL helped conduct the animal study. All of the authors reviewed the manuscript before submission and approved the final manuscript.

Funding

This work was supported by grants from the National Natural Science Foundation of China (NSFC) (Grant Number: 81702769), CAMS Innovation Fund for Medical Science (No. 2017-I2M-1-016), and the PUMC Youth Fund (Grant Number: 3332017105).

Availability of data and materials

All data generated or analyzed during this study are included either in this article or in the supplementary information files.

Ethics approval and consent to participate

The study was approved by the Medical Ethics Committee of the Institute of Microcirculation, CAMS & PUMC.

Consent for publication

All authors agree on publication of the results of the present manuscript.

Competing interests

The authors declare that they have no competing interests.

References

1. Bai J, Li Y, Zhang G. Cell cycle regulation and anticancer drug discovery. Cancer Biol Med. 2017;14(4):348-62.
2. Thu KL, Soria-Bretones I, Mak TW, Cescon DW. Targeting the cell cycle in breast cancer: towards the next phase. Cell Cycle. 2018;17(15):1871-85.
3. Pandey K, An HJ, Kim SK, Lee SA, Kim S, Lim SM, et al. Molecular mechanisms of resistance to CDK4/6 inhibitors in breast cancer: A review. Int J Cancer. 2019;145(5):1179-88.
4. Vinuesa CG, Cook MC, Angelucci C, Athanasopoulos V, Rui L, Hill KM, et al. A RING-type ubiquitin ligase family member required to repress follicular helper T cells and autoimmunity. Nature. 2005;435(7041):452-8.
5. Yu D, Tan AH, Hu X, Athanasopoulos V, Simpson N, Silva DG, et al. Roquin represses autoimmunity by limiting inducible T-cell co-stimulator messenger RNA. Nature. 2007;450(7167):299-303.
6. Schaefer JS, Montufar-Solis D, Klein JR. A role for IL-10 in the transcriptional regulation of Roquin-1. Gene. 2014;549(1):134-40.
7. Glasmacher E, Hoefig KP, Vogel KU, Rath N, Du L, Wolf C, et al. Roquin binds inducible costimulator mRNA and effectors of mRNA decay to induce microRNA-independent post-transcriptional repression. Nat Immunol. 2010;11(8):725-33.
8. Heissmeyer V, Vogel KU. Molecular control of Tfh-cell differentiation by Roquin family proteins. Immunol Rev. 2013;253(1):273-89.
9. Drees C, Vahl JC, Bortoluzzi S, Heger KD, Fischer JC, Wunderlich FT, et al. Roquin Paralogs Differentially Regulate Functional NKT Cell Subsets. J Immunol. 2017;198(7):2747-59.
10. Lee SY, Lee SH, Seo HB, Ryu JG, Jung K, Choi JW, et al. Inhibition of IL-17 ameliorates systemic lupus erythematosus in Roquin(san/san) mice through regulating the balance of TFH cells, GC B cells, Treg and Breg. Sci Rep. 2019;9(1):5227.
11. Bertossi A, Aichinger M, Sansonetti P, Lech M, Neff F, Pal M, et al. Loss of Roquin induces early death and immune deregulation but not autoimmunity. J Exp Med. 2011;208(9):1749-56.
12. Schaefer JS, Montufar-Solis D, Nakra N, Vigneswaran N, Klein JR. Small intestine inflammation in Roquin-mutant and Roquin-deficient mice. PLoS One. 2013;8(2):e56436.
13. Schuetz A, Murakawa Y, Rosenbaum E, Landthaler M, Heinemann U. Roquin binding to target mRNAs involves a winged helix-turn-helix motif. Nat Commun. 2014;5:5701.
14. Janowski R, Heinz GA, Schlundt A, Wommelsdorf N, Brenner S, Gruber AR, et al. Roquin recognizes a non-canonical hexaloop structure in the 3'-UTR of Ox40. Nat Commun. 2016;7:11032.
15. Braun J, Fischer S, Xu ZZ, Sun H, Ghoneim DH, Gimbel AT, et al. Identification of new high affinity targets for Roquin based on structural conservation. Nucleic Acids Res. 2018;46(22):12109-25.
16. Ramiscal RR, Parish IA, Lee-Young RS, Babon JJ, Blagih J, Pratama A, et al. Attenuation of AMPK signaling by ROQUIN promotes T follicular helper cell formation. Elife. 2015;4.

17. Murakawa Y, Hinz M, Mothes J, Schuetz A, Uhl M, Wyler E, et al. RC3H1 post-transcriptionally regulates A20 mRNA and modulates the activity of the IKK/NF-kappaB pathway. Nat Commun. 2015;6:7367.
18. Essig K, Hu D, Guimaraes JC, Alterauge D, Edelmann S, Raj T, et al. Roquin Suppresses the PI3K-mTOR Signaling Pathway to Inhibit T Helper Cell Differentiation and Conversion of Treg to Tfr Cells. Immunity. 2017;47(6):1067-82 e12.
19. Srivastava M, Duan G, Kershaw NJ, Athanasopoulos V, Yeo JH, Ose T, et al. Roquin binds microRNA-146a and Argonaute2 to regulate microRNA homeostasis. Nat Commun. 2015;6:6253.
20. Auguste T, Travert M, Tarte K, Ame-Thomas P, Artchounin C, Martin-Garcia N, et al. ROQUIN/RC3H1 alterations are not found in angioimmunoblastic T-cell lymphoma. PLoS One. 2013;8(6):e64536.
21. Gyorffy B, Lanczky A, Eklund AC, Denkert C, Budczies J, Li Q, et al. An online survival analysis tool to rapidly assess the effect of 22,277 genes on breast cancer prognosis using microarray data of 1,809 patients. Breast Cancer Res Treat. 2010;123(3):725-31.
22. Lu W, Ning H, Gu L, Peng H, Wang Q, Hou R, et al. MCPIP1 Selectively Destabilizes Transcripts Associated with an Antiapoptotic Gene Expression Program in Breast Cancer Cells That Can Elicit Complete Tumor Regression. Cancer Res. 2016;76(6):1429-40.
23. Mino T, Murakawa Y, Fukao A, Vandenbon A, Wessels HH, Ori D, et al. Regnase-1 and Roquin Regulate a Common Element in Inflammatory mRNAs by Spatiotemporally Distinct Mechanisms. Cell. 2015;161(5):1058-73.
24. Schlundt A, Heinz GA, Janowski R, Geerlof A, Stehle R, Heissmeyer V, et al. Structural basis for RNA recognition in roquin-mediated post-transcriptional gene regulation. Nat Struct Mol Biol. 2014;21(8):671-8.
25. Hofacker IL. Vienna RNA secondary structure server. Nucleic Acids Res. 2003;31(13):3429-31.
26. Wu Y, Zheng Q, Li Y, Wang G, Gao S, Zhang X, et al. Metformin targets a YAP1-TEAD4 complex via AMPKalpha to regulate CCNE1/2 in bladder cancer cells. J Exp Clin Cancer Res. 2019;38(1):376.
27. Tyagi N, Deshmukh SK, Srivastava SK, Azim S, Ahmad A, Al-Ghadhban A, et al. ETV4 Facilitates Cell-Cycle Progression in Pancreatic Cells through Transcriptional Regulation of Cyclin D1. Mol Cancer Res. 2018;16(2):187-96.
28. Ingham M, Schwartz GK. Cell-Cycle Therapeutics Come of Age. J Clin Oncol. 2017;35(25):2949-59.
29. Zhang X, Teng Y, Yang F, Wang M, Hong X, Ye LG, et al. MCM2 is a therapeutic target of lovastatin in human non-small cell lung carcinomas. Oncol Rep. 2015;33(5):2599-605.
30. Ouhara K, Munenaga S, Kajiya M, Takeda K, Matsuda S, Sato Y, et al. The induced RNA-binding protein, HuR, targets 3'-UTR region of IL-6 mRNA and enhances its stabilization in periodontitis. Clin Exp Immunol. 2018;192(3):325-36.
31. Kim DJ, Vo MT, Choi SH, Lee JH, Jeong SY, Hong CH, et al. Tristetraprolin-mediated hexokinase 2 expression regulation contributes to glycolysis in cancer cells. Mol Biol Cell. 2019;30(5):542-53.

32. Tan D, Zhou M, Kiledjian M, Tong L. The ROQ domain of Roquin recognizes mRNA constitutive-decay element and double-stranded RNA. Nat Struct Mol Biol. 2014;21(8):679-85.
33. Khabar KS. Post-transcriptional control during chronic inflammation and cancer: a focus on AU-rich elements. Cell Mol Life Sci. 2010;67(17):2937-55.
34. Vlasova IA, Tahoe NM, Fan D, Larsson O, Rattenbacher B, Sternjohn JR, et al. Conserved GU-rich elements mediate mRNA decay by binding to CUG-binding protein 1. Mol Cell. 2008;29(2):263-70.
35. Li M, Cao W, Liu H, Zhang W, Liu X, Cai Z, et al. MCPIP1 down-regulates IL-2 expression through an ARE-independent pathway. PLoS One. 2012;7(11):e49841.
36. Sgromo A, Raisch T, Bawankar P, Bhandari D, Chen Y, Kuzuoglu-Ozturk D, et al. A CAF40-binding motif facilitates recruitment of the CCR4-NOT complex to mRNAs targeted by Drosophila Roquin. Nat Commun. 2017;8:14307.
37. Leppek K, Schott J, Reitter S, Poetz F, Hammond MC, Stoecklin G. Roquin promotes constitutive mRNA decay via a conserved class of stem-loop recognition motifs. Cell. 2013;153(4):869-81.

Figures

Figure 1

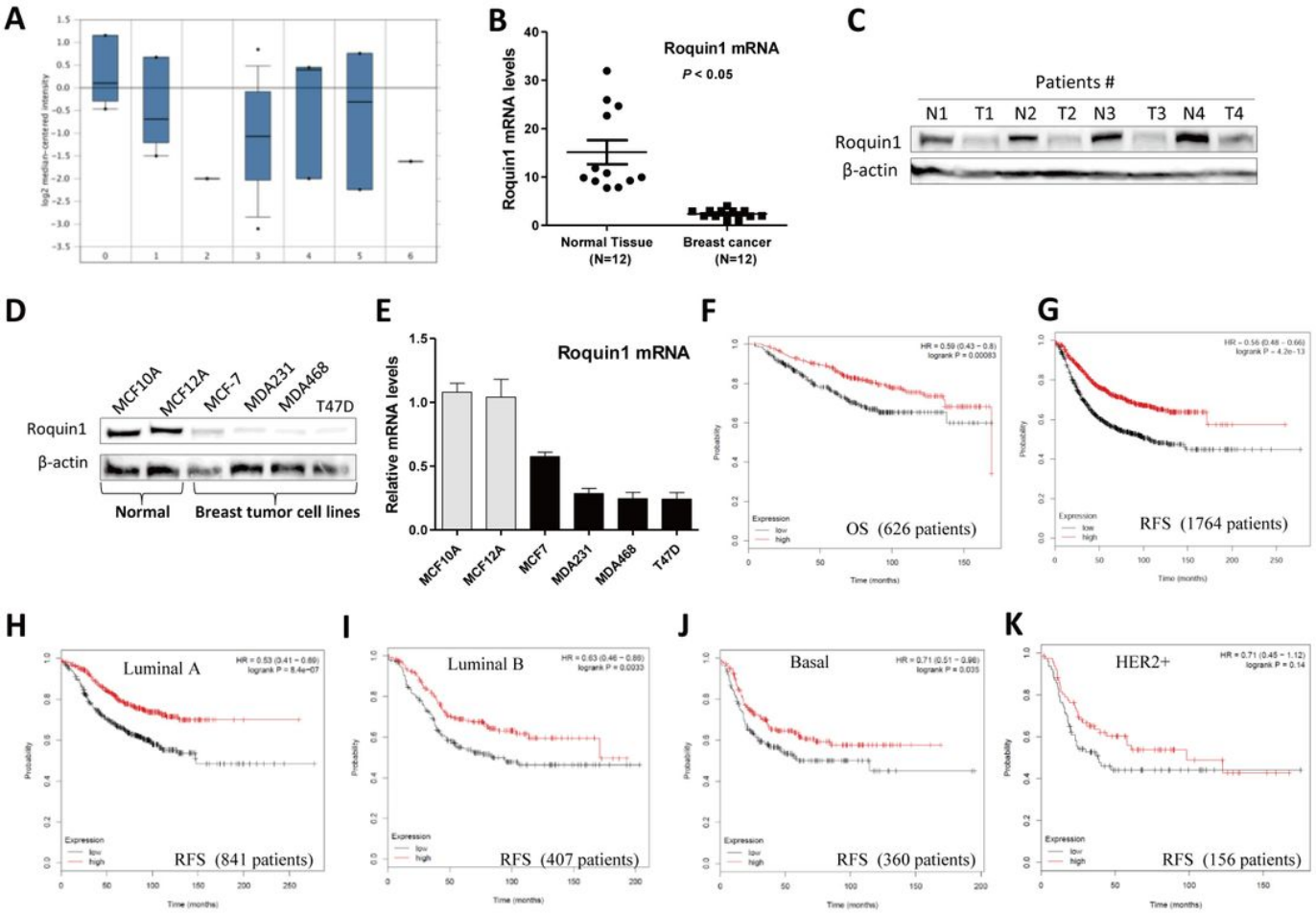

Figure 1

Roquin1 expression was reduced in breast cancer patients and was associated with poor survival. a Roquin1 mRNA expression among normal (0) (n = 4), breast carcinoma (1) (n = 4), ductal breast carcinoma in situ (2) (n = 1), invasive ductal breast carcinoma (3) (n = 18), invasive lobular breast carcinoma (4) (n = 3), invasive mixed breast carcinoma (5) (n = 3), and male breast carcinoma (6) (n = 1). b Roquin1 expression was measured by qPCR in human breast tumor specimens (n = 12) compared with surrounding “normal” breast tissue (n = 12). c Roquin1 protein level was measured in human breast tumor tissues and normal mammary gland tissues. d-e Roquin1 protein (d) and mRNA (e) levels were measured by Western blot analysis and qPCR in human breast tumor cell lines and human normal mammary gland epithelial cell lines, respectively. f-g Kaplan–Meier overall survival (f) and relapse-free survival (g) curves of patients with breast tumors having low and high tumor Roquin1 transcripts. h–k Kaplan–Meier relapse-free survival curves of patients with luminal A (h), luminal B (i), basal (j), and Her2+ (k) breast tumor having low and high tumor Roquin1 transcripts.

Figure 2

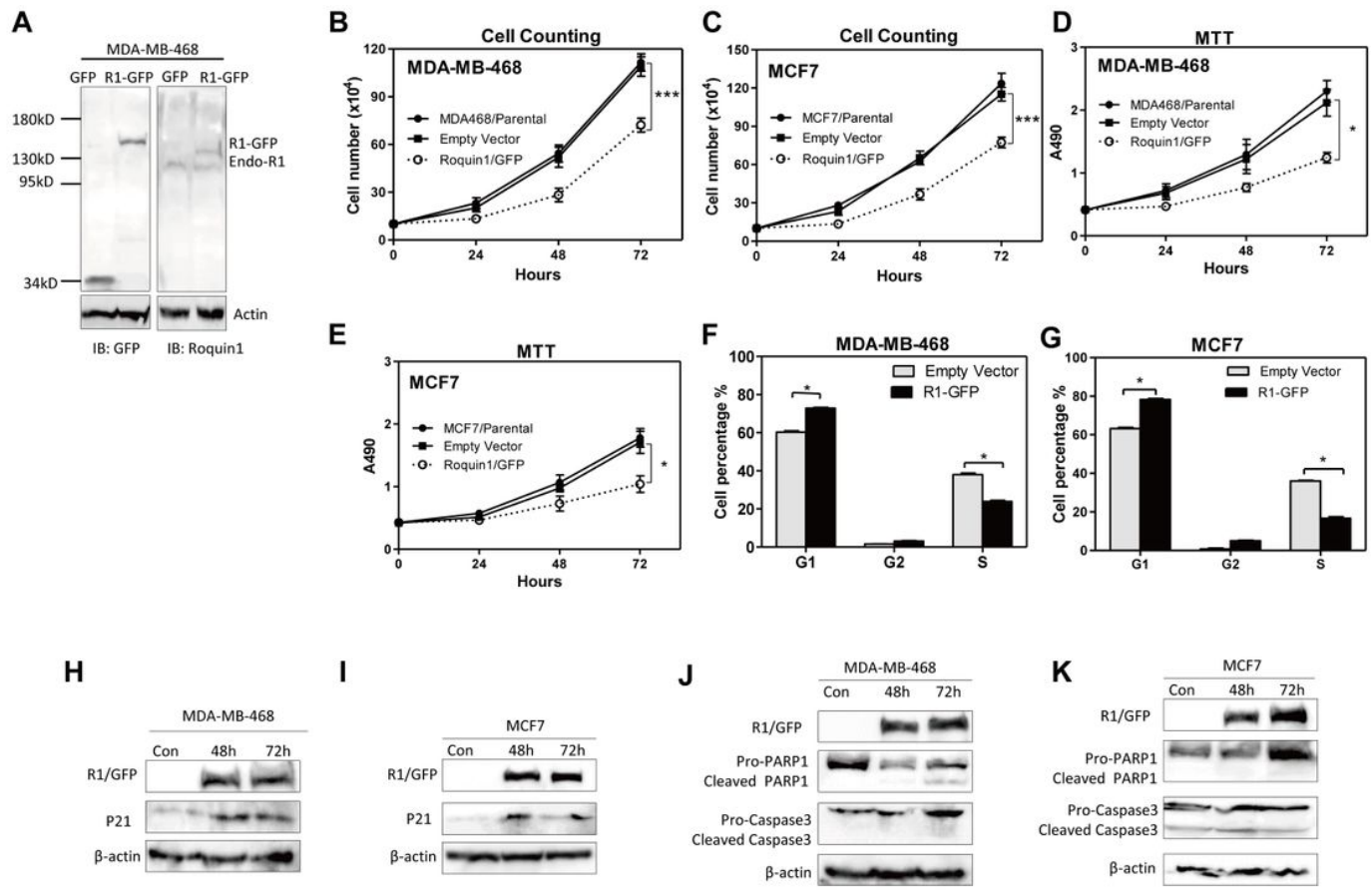

Figure 2

Roquin1 inhibits cell proliferation and induced G1/S phase cell cycle arrest in breast cancer cells. a Roquin1/GFP fusion protein was detected by immunoblotting with anti-GFP and anti-Roquin1 antibodies, respectively. b-c Cell counting were conducted to measure the growth of MDA-MB-468 (b) and MCF7 (c) cells after the overexpression of Roquin1/GFP (n = 3). ***P < 0.0001. d-e MTT assay was performed to measure the cell activity of MDA-MB-468 (d) and MCF7 (e) cells overexpressing Roquin1/GFP protein (n = 3). *P < 0.05. f-g Cell cycle was analyzed by FCM in MDA-MB-468 (f) and MCF7 (g) cells after Roquin1 overexpression. The proportions of cells in the G1, G2, and S phases are shown (n = 3). *P < 0.05. h-i p21 protein was detected by immunoblotting with an anti-p21 antibody at different time points after Roquin1 overexpression in MDA-MB-468 (h) and MCF-7 (i) cells. j-k Apoptosis indicators PARP-1 and caspase-3 were measured by immunoblotting at different time points after Roquin1 overexpression in MDA-MB-468 (j) and MCF-7 (k) cells, respectively.

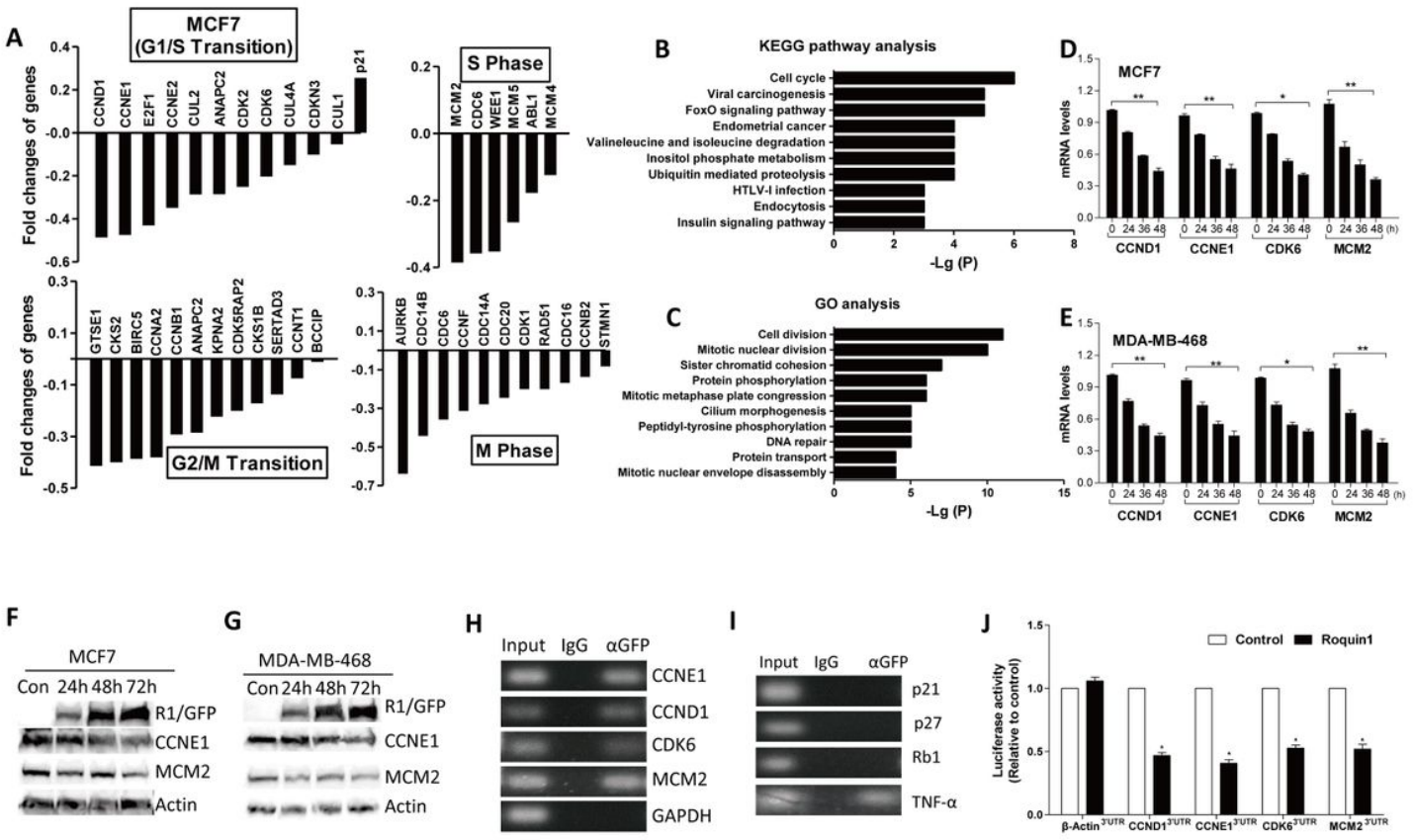

Figure 3

Roquin1 selectively inhibited the mRNA expression of cell cycle–promoting genes via targeting the 3′UTR. a RNA-seq analysis showed changes in the expression levels of cell cycle–related genes by Roquin1 in MCF7 cells. The genes promoting G1/S, S phase, G2/M, and M phase transition were downregulated; and the expression of cell cycle progression inhibitor p21 was upregulated. b Top 10 KEGG pathways enriched for common downregulated genes of Roquin1. c Top 10 GO terms (biological processes) for the analysis for common downregulated genes. d-e The mRNA levels of indicated cell cycle–promoting genes were measured by qPCR in MCF7 (d) and MDA-MB-468 (e) cells at indicated time points. *P < 0.05; **P < 0.01 between two groups. f-g CCNE1 and MCM2 were measured by immunoblotting with anti-CCNE1 and anti-MCM2 antibodies at different time points after Roquin1 overexpression in MCF7 (f) and MDA-MB-468 (g) cells. h-i Roquin1/GFP fusion protein were expressed in MDA-MB-468 cells, after lysate extraction, immunoprecipitation with anti-GFP antibody or IgG, and RNA extraction. Cell cycle–promoting gene (h) and –inhibiting gene (i) transcripts were detected by RT-PCR. j Measurement of luciferase activity of reporters containing the 3′UTRs of CCND1, CCNE1, CKD6 (part),

and MCM2, respectively. β-Actin 3′UTR was used as a negative control. The results shown represent the mean ± standard deviation of four independent experiments. *P < 0.05

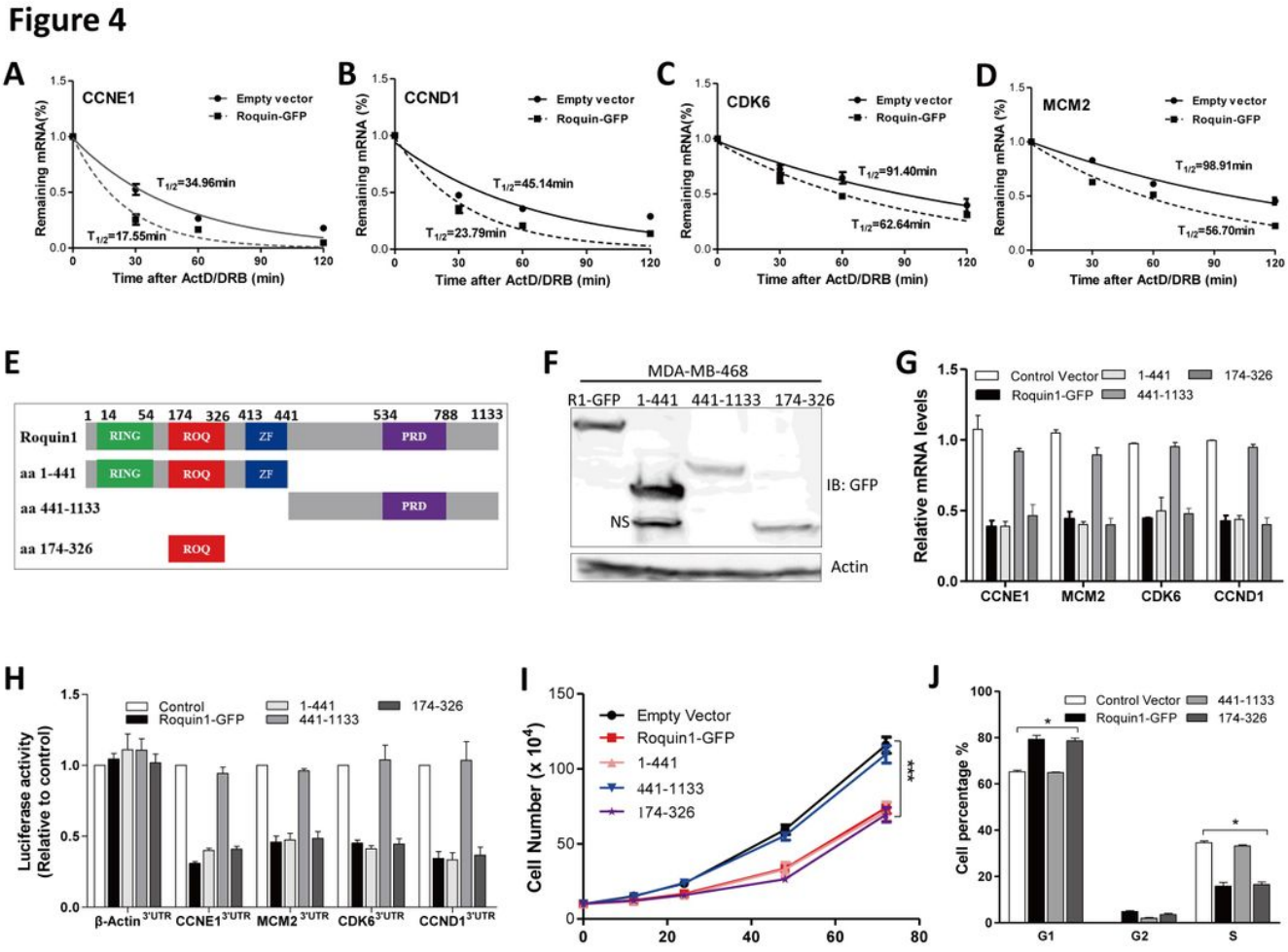

Figure 4

Roquin1 destabilized the mRNAs of cell cycle–promoting genes via the ROQ domain. a–d MDA-MB-468 cells overexpressing Roquin1/GFP protein were added with ActD and DRB for different time points. The levels of remaining cell cycle–promoting gene transcripts, including CCND1 (a), CCNE1 (b), CDK6 (c), and MCM2 (d), were measured by qPCR. e Schematic representation of the ROQ, RING, zinc finger (ZF), and PRD domains in Roquin1, and their truncations: aa 1-441, aa 441-1133, and aa 174-326. f Expression of Roquin1/GFP and its truncated mutations were confirmed by immunoblotting with an anti-GFP antibody. g MDA-MB-468 cells were transiently transfected with Roquin1 and its mutants. After 36 hours, total RNA was extracted to measure the mRNA expression of indicated genes by qPCR. h HEK293 cells were co-transfected with indicated reporters and Roquin1 as well as its truncations. After 36 hours, luciferase activity was measured in cell lysates and compared with that cells transfected with empty vector. i Cell counting was conducted in MDA-MB-468 cells after overexpressing Roquin1 and its mutants (n = 3). ***P

< 0.0001. j Cell cycle was examined by FCM in MDA-MB-468 cells after overexpressing Roquin1 and its mutants (n = 3). *P < 0.05

Figure 5

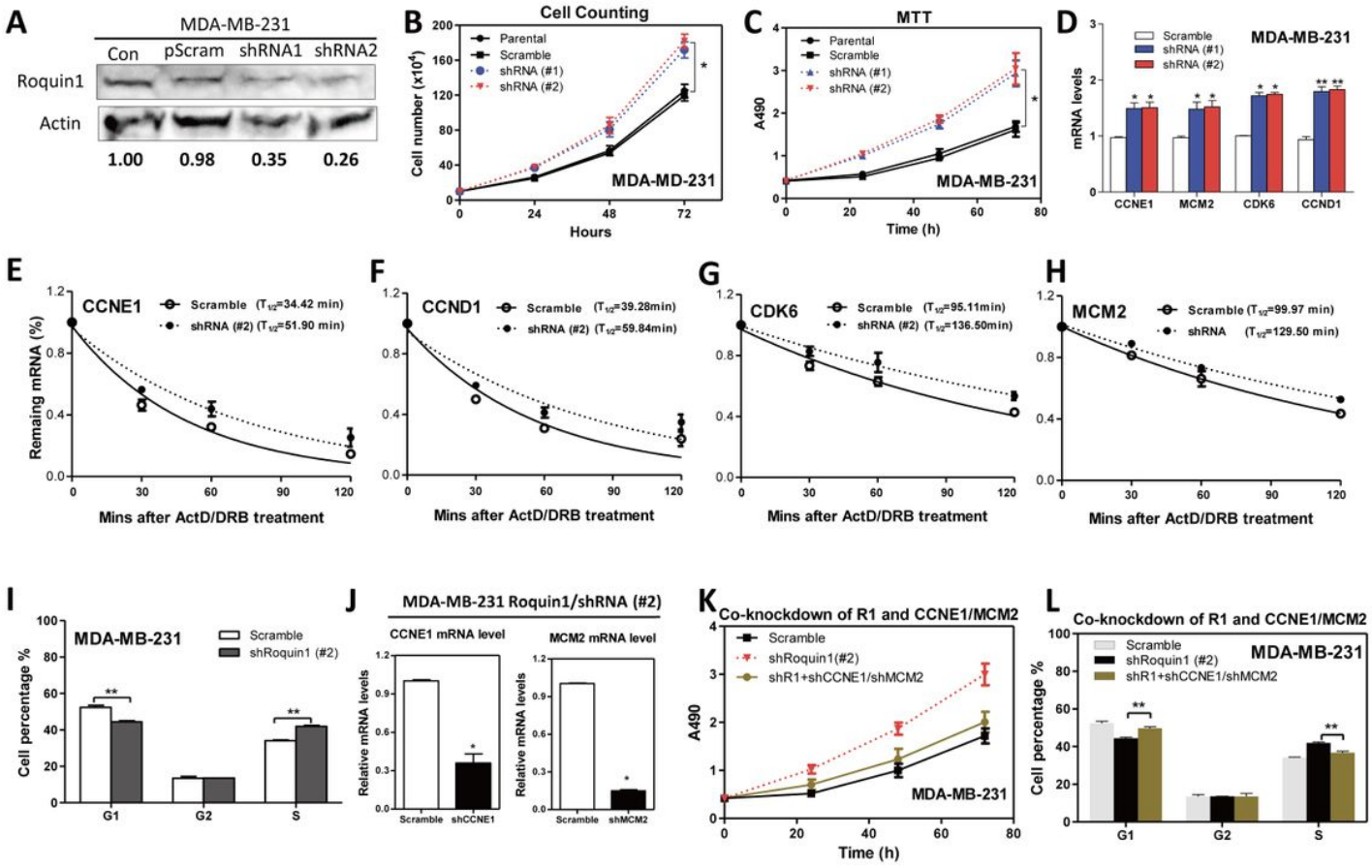

Figure 5

Roquin1 knockdown stabilized cell cycle–promoting gene transcripts and promoted G1/S cell cycle progression. a Roquin1 knockdown was validated by western blot analysis. b-c Cell proliferation was measured by cell counting (b) and MTT assay (c) in MDA-MB-231 cells after knocking down Roquin1 at the indicated time points (n = 3). *P < 0.05. d Cell cycle–promoting gene mRNAs were measured in the Roquin1 knocked down MDA-MB-231 cells by qPCR. **P < 0.01 between two groups. e–h The half-lives of cell cycle–promoting genes were measured in Roquin1 knockdown MDA-MB-231 cells. i Cell cycle analysis was performed in MDA-MB-231 cells after the knockdown of Roquin1. The proportions of cells in the G1, G2, and S phases are shown (n = 3). **P < 0.01. j MDA-MB-231/Roquin1-knockdown cells were infected with scramble/lentivirus or shRNA lentivirus targeting CCNE1 and MCM2, respectively. Total RNA was extracted to measure the levels of mRNAs of CCNE1 and MCM2. *P < 0.05. k MTT assay was conducted to measure the cell growth of MDA-MB-231 cells after the co-knockdown of Roquin1 and

CCNE1/MCM2. l Cell cycle analysis was performed in MDA-MB-231 cells after the co-knockdown of Roquin1 and CCNE1/MCM2. **P < 0.01

Figure 6

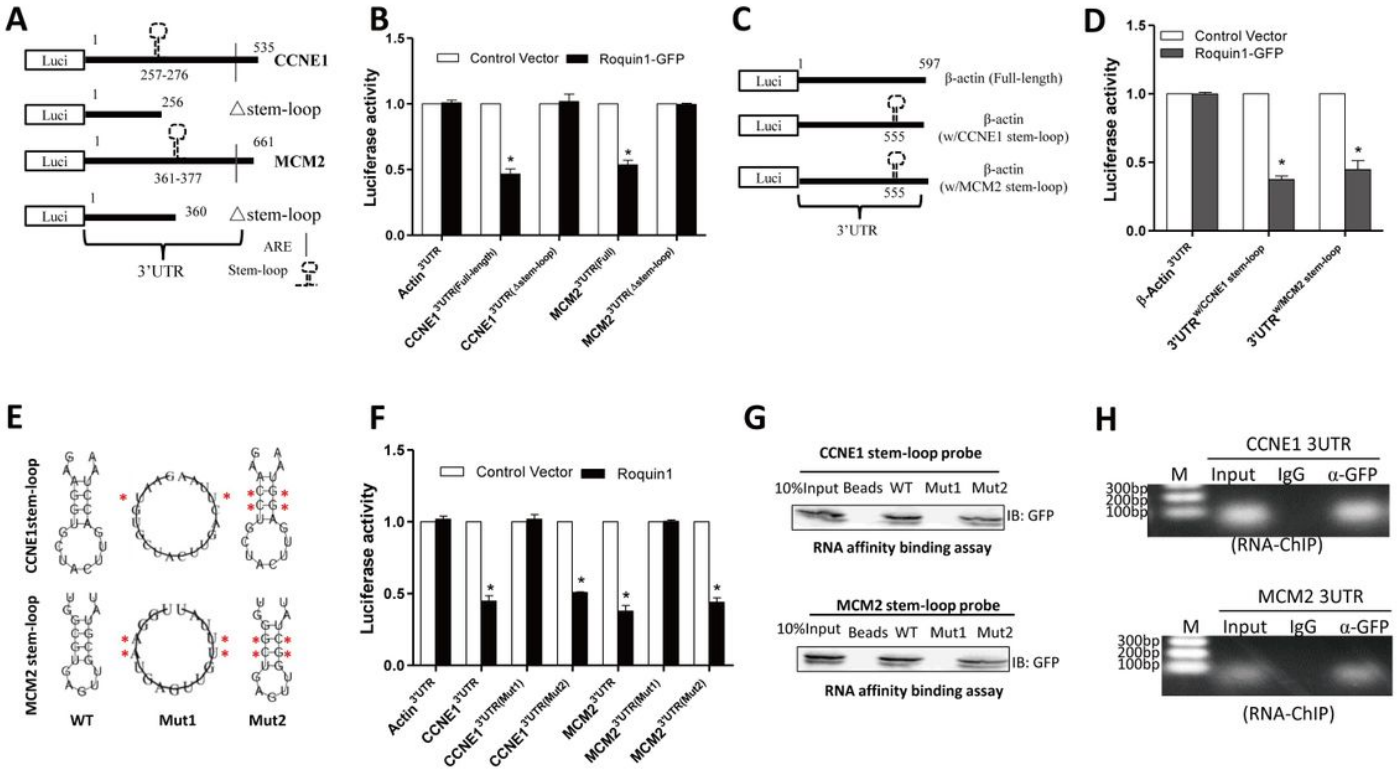

Figure 6

Roquin1 bound to the stem–loop structure in the 3′UTR of cell cycle–promoting genes a Schematic representation of the luciferase reporter constructs of CCNE1 and MCM2 containing truncated 3′UTRs without the stem–loop structure (Δ stem–loop). b Measurement of luciferase activity of reporters containing full-length 3′UTRs or truncated 3′UTRs (Δ stem–loop) of CCNE1 and MCM2, respectively. The results shown represent the mean ± standard deviation of four independent experiments. *P < 0.05. c Schematic representation of the luciferase reporter constructs of human β-actin 3′UTR containing the stem–loop structure of CCNE1 (w/CCNE1 stem–loop) or MCM2 (w/MCM2 stem–loop). d Measurement of luciferase activity of reporters containing wild-type β-actin 3′UTRs or β-actin 3′UTRs with stem-loop sequences of CCNE1 and MCM2. *P < 0.05. e The predicted stem–loop structures of CCNE1 (top) and MCM2 (bottom) in their 3′UTRs and mutation strategy (asterisks indicate base substitution). Mutant1 was unable to form a stem–loop structure (middle), and Mutant2 still formed a stem–loop structure (left). f Luciferase assays were conducted using reporters from (E) along with Roquin1 or control vector,

and then measurement of the luciferase activity. *P < 0.05. g Roquin1/GFP fusion protein was expressed in MDA-MB-231 cells for 24 hours, and then cell lysates were collected. Biotinylated CCNE1 and MCM2 wild-type or mutant probes (mut1 and mut2) were used for the pull-down assay. h RIP-ChIP assay was conducted with genome fragments from MDA-MB-231 cells after Roquin1/GFP fusion protein expression for 24 hours.

Figure 7

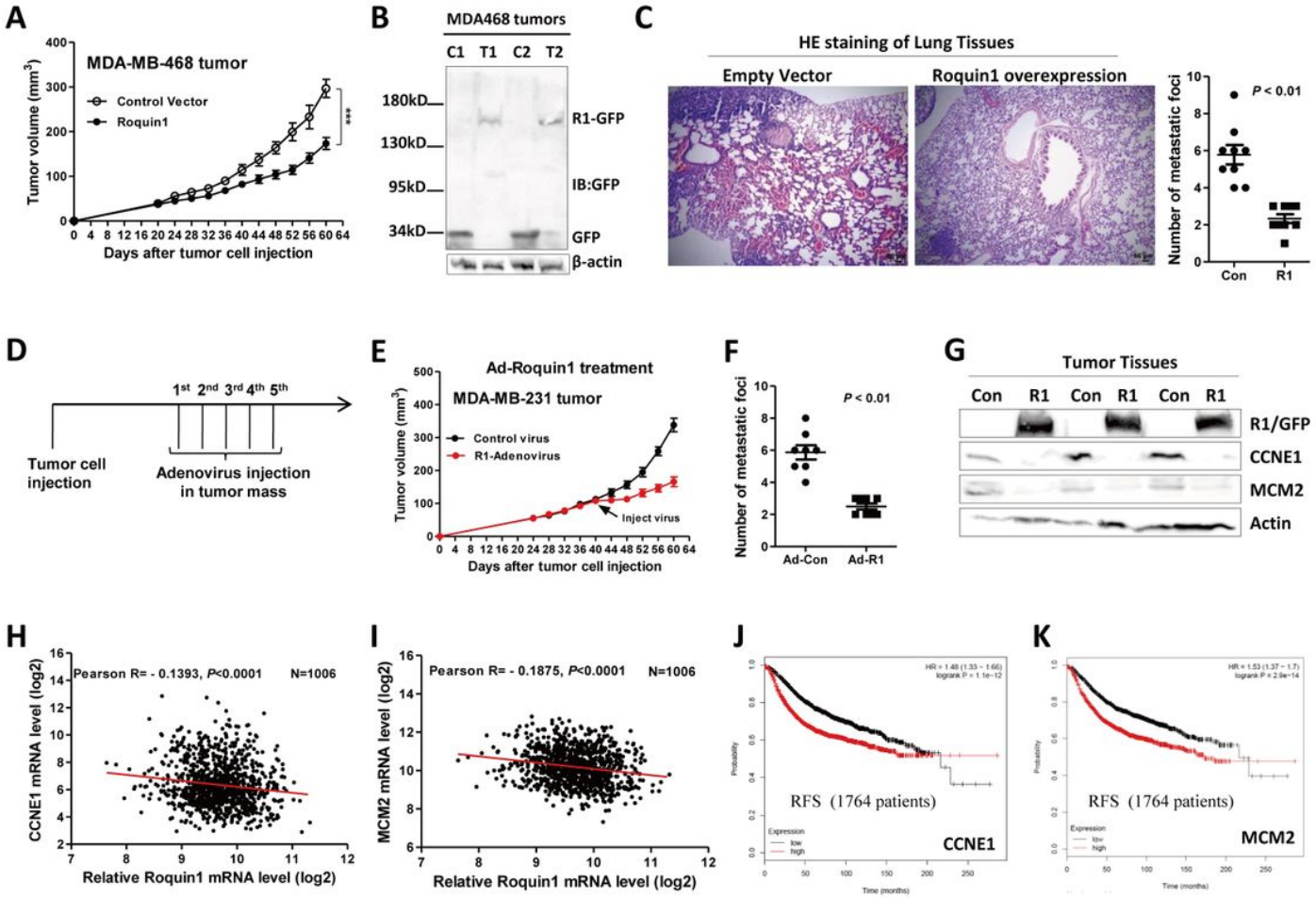

Figure 7

Roquin1 suppressed breast tumor growth and metastasis. a Tumor growth curves in nude mice received 5 × 106 MDA-MB-468/Roquin-GFP and MDA-MB-468/GFP cells (n = 4/group). ***P < 0.0001 between two groups. b Total protein was extracted from tumor tissues and used to detect Roquin1/GFP expression by immunoblotting with an anti-GFP antibody. c H&E staining of lung tissue sections from nude mice bearing MDA-MB-468/GFP or MDA-MB-468/Roquin1–GFP tumors. Scale bar, 50 μm. d Experimental flow chart for tumor treatment with Roquin1-expressing adenovirus in vivo. MDA-MB-231 cells (3 × 106 cells/100 μL of PBS) were injected into nude mice to establish a tumor mass. Tumors were treated with adenovirus (109 PFU adenovirus in 100 μL of PBS) every other day when tumors grew to a certain size (~5 mm in diameter). e Tumor growth curves in nude mice after treatment with adenovirus. Black arrows

indicate the time point of adenovirus injection. f Quantification of the number of metastatic foci of each mouse treated with control or Roquin1-expressing adenovirus. g Total protein was extracted from tumor tissues to detect the expression of Roquin1/GFP, CCNE1, and MCM2 by immunoblotting with anti-GFP, anti-CCNE1, and anti-MCM2 antibodies, respectively. β-actin was used as a loading control. h-i Pearson's Correlation analysis between Roquin1 and CCNE1 (h) and MCM2 (i) expression levels in log2 values in human breast cancer patients (n = 1006). j-k Kaplan–Meier relapse-free survival curves of patients with breast cancer having low and high levels of tumor CCNE1 (j) and MCM2 (k) transcripts.

Supplementary Files

This is a list of supplementary files associated with this preprint. Click to download.

- Additionalfile5TableS3Sequencesofprimersandprobes.docx
- Additionalfile4TableS2Roquin1CCNE1andMCM2inBRCA.xlsx
- Additionalfile3TableS1RNAseqdata.xlsx
- Additionalfile2SupplementaryMaterialsandMethods.docx
- Additionalfile1FigureS1S7.docx